JOURNAL OF MATERIALS SCIENCE 24 (1989) 3196–3204

# Apparent activation volume for creep of copper and alpha brass at intermediate temperatures

S. V. RAJ
*NASA Lewis Research Center, MS 49-1, 21000 Brookpark Road, Cleveland, Ohio 44135, USA*

Experimental measurements of the apparent activation volume for creep, $V^*$, of Cu and Cu–30% Zn conducted at intermediate temperatures showed two types of strain dependencies. At the lower temperatures and higher stresses, $V^*$ decreased with increasing creep strain, $\varepsilon$, while at higher temperatures and lower stresses, $V^*$ was essentially independent of strain. The low temperature–high stress behaviour for Cu and Cu–30% Zn was found to be consistent with the dominance of a dislocation intersection mechanism. The high temperature–low stress data for the pure metals suggest that the rate-controlling process involves the nonconservative motion of jogs on screw dislocations. For the latter conditions, an additional contribution from solute drag-limited dislocation glide also appears to be important in governing the creep behaviour of the alloy.

## 1. Introduction

Under conditions when a single creep mechanism is dominant, the shear strain rate, $\dot{\gamma}$, is described by

$$\dot{\gamma} = \dot{\gamma}_0 \exp(-\Delta G_c/kT) \quad (1)$$

where $\Delta G_c$ is the stress and pressure dependent Gibbs minimum free energy for creep, $k$ is Boltzmann's constant, $T$ is the absolute temperature, and $\dot{\gamma}_0$ is the maximum shear strain rate.

Li and co-workers [1–3] first suggested the possibility of using Equation 1 to derive a complete set of activation parameters from creep data. For a single rate-controlling process and for a constant value of $\dot{\gamma}_0$, it follows from Equation 1 that [1, 2, 4, 5]

$$\left[\frac{\partial \ln \dot{\gamma}}{\partial T}\right]_{\tau,P} = \frac{1}{kT^2}\left[\frac{\partial(\Delta G_c/T)}{\partial(1/T)}\right]_{\tau,P} = \frac{\Delta H}{kT^2} \quad (2)$$

$$\left[\frac{\partial \ln \dot{\gamma}}{\partial P}\right]_{\tau,T} = -\frac{1}{kT}\left[\frac{\partial \Delta G_c}{\partial P}\right]_{\tau,P} = -\frac{\Delta V}{kT} \quad (3)$$

$$\left[\frac{\partial \ln \dot{\gamma}}{\partial \tau}\right]_{P,T} = -\frac{1}{kT}\left[\frac{\partial \Delta G_c}{\partial \tau}\right]_{P,T} = \frac{A^* b}{kT} \quad (4)$$

where $\tau$ is the shear stress, $\Delta H$ is the activation enthalpy for creep, $P$ is the hydrostatic pressure, $\Delta V$ and $A^*$ are the true activation volume and activation area for creep, respectively and $\boldsymbol{b}$ is the Burgers vector. A knowledge of the three activation parameters, $\Delta H$, $\Delta V$, and $A^*$ is useful in identifying the dominant creep mechanism for a given combination of stress, pressure, and temperature. For example, when the creep mechanism is diffusion controlled, $\Delta H \approx \Delta H_{SD}$ and $\Delta V \approx \Delta V_{SD}$ [6–8], where $\Delta H_{SD}$ and $\Delta V_{SD}$ are the activation energy and activation volume for self diffusion, respectively, while for the specific case involving Nabarro–Herring creep or the climb of a single edge dislocation, $A^* \approx \boldsymbol{b}^2$ [2–5].

The experimental determination of $\Delta V$ is complex, and other than for geological materials, it is rarely measured in practice. By comparison, measurements of $\Delta H$ and $A^*$ are relatively simple and generally provide sufficient information regarding the rate-controlling mechanism. However, in most instances, the dominant mechanisms operating at intermediate (typically, 0.3 to 0.7 $T_m$, where $T_m$ is the absolute melting point) and high temperatures are identified on the basis of the stress exponent, $n$, and the activation energy for creep, $Q_c$ (i.e. $\Delta H$), and there are relatively few reported measurements of $A^*$. Although measurements of $n$ and $Q_c$ are generally useful in identifying rate-controlling mechanisms which can be described by a power-law relation between the creep rate and the applied stress, they are inadequate when this relationship is no longer valid. This is, of course, true when the exponential creep law is known to be valid.

Unfortunately, the exponential relation is not always easily discerned from double logarithmic plots of the creep rate against the applied stress because a power-law relation with $n > 4.5$ can often represent the experimental data fairly well. This is especially true when the data vary over a limited range of creep rates (typically, less than five orders of magnitude) and temperatures, or lie in the transition region between power-law and exponential creep. For example, a recent analysis of creep data on several fcc metals suggests that values of $n > 4.5$ correspond to the power-law breakdown region [9]. In such instances, an interpretation of the experimental results based merely on the values of $n$ and $Q_c$ can lead to erroneous conclusions regarding the rate-controlling process unless experimental measurements of $A^*$ also compliment the final analyses. Additionally, experimental determinations of $A^*$ or the apparent activation volume, $V^*$, (i.e. $A^*b$) in the power-law creep regime,



0022–2461/89 $03.00 + .12 

TABLE I Semi-quantitative spectrographic analyses (wt %) and the initial condition of the test materials

| Material | Chemical composition | | | | | | | | | | | Initial condition |
|---|---|---|---|---|---|---|---|---|---|---|---|---|
| | Al | Ag | Cu | Fe | Mg | Ni | O | Pb | Si | Sn | Zn | |
| Al | Bal. | – | 0.0020 | – | 0.0020 | – | – | – | 0.0010 | – | – | 12.7 mm diameter cold-worked rods |
| Cu | – | 0.0010 | Bal. | 0.005 | – | – | 0.0152 | – | – | – | – | 3 mm thick hot-rolled sheets. Grain size: 12 ± 2 μm |
| Cu–30% Zn | 0.0010 | 0.0050 | 69.4 | 0.0200 | – | 0.0150 | 0.0023 | 0.0050 | – | 0.0100 | 30.5 | 2 mm thick hot-rolled sheets. Grain size: 12 ± 2 μm. |

where dislocation climb is important, can provide valuable information regarding whether the process involves the climb of single-edge dislocations or the nonconservative motion of jogs on screw dislocations. In particular, values of $A^*$ or $V^*$ can be used in evaluating the force–distance diagram for the dominant process.

The current investigation was undertaken as part of an overall effort to understand the creep behaviour of copper and Cu–30% Zn in the intermediate temperature region. In the case of copper, a compilation of experimental data from several sources revealed large discrepancies in the reported values of the activation energy [10]. Similarly, a review of published results on alpha brass suggested that class A behaviour may be dominant under certain circumstances [11], although this material is usually classified as a class M alloy [6]. The present paper reports the results of experiments carried out to measure the apparent activation volumes for copper and alpha brass in order to compliment other data and analyses on these materials [11]. Some experimental measurements of $V^*$ were also carried out on pure aluminium under conditions when dislocation climb is known to be dominant [12], and these are reported primarily to aid in the interpretation of the data on the other two materials studied in this investigation.

## 2. Experimental details

The chemical composition and the initial conditions of the three materials used in this investigation are given in Table I. Hot-rolled sheets of copper and alpha brass of dimensions 305 mm × 150 mm × 3 mm and 305 mm × 100 mm × 2 mm, respectively, were supplied by the Olin Corporation, and flat tensile specimens were machined from them with a gauge length of 25.4 mm and a gauge width of 9.5 mm. The aluminium specimens were machined from 12.7 mm diameter rods, and these had a gauge length of about 25.4 mm and a gauge diameter of 6.3 mm. The axis of each specimen was along the rolling or the swaging directions in all cases, and the variation in the specimen dimensions was less than 0.5%. The specimens were annealed in argon, and the heat-treatment conditions used for each material are given in Table II. Fairly reproducible and equiaxed grains were obtained from these heat treatments, and the average values of the linear intercept grain size, determined from a statistical sample size of 500 to 1000 grains, are also included in Table II.

TABLE II Annealing treatments and the final grain sizes of the test materials

| Material | Temperature* (K) | Time (h) | Grain Size† (μm) |
|---|---|---|---|
| Aluminium | 773 ± 1 | 0.25 | 230 ± 25 |
| Copper | 1073 ± 1 | 2.0 | 250 ± 15 |
| Cu–30% Zn | 923 ± 1 | 6.0 | 120 ± 10 |

*All specimens were annealed in argon.
†These values represent the average linear intercept grain size obtained from a statistical sample size of 500 to 1000 grains. The errors represent the 95% confidence limit.

Constant stress creep tests were conducted under a flowing argon atmosphere maintained at a slightly positive pressure. The actual details of the testing procedure are described elsewhere [10, 11]. Specimens were tested in the intermediate temperature range from 623 to 973 K (0.46 to 0.72 $T_m$) for copper and 573 to 823 K (0.48 to 0.70 $T_m$) for alpha brass with a temperature control better than ± 1 K. The temperature gradient over the specimen gauge length during testing was less than 1 K, and the accuracy of strain measurement was generally about $10^{-4}$ and the strain resolution was about $5 \times 10^{-5}$.

The apparent activation volume for creep was determined by measuring the creep rates before and after small stress changes ($\sim 0.05\ \sigma$, where $\sigma$ is the applied normal stress) at various testing temperatures. The technique is demonstrated in Figs 1 and 2 which show typical chart recordings of strain, $\varepsilon$, and time, $t$, for Cu–30% Zn after a stress increase and a stress decrease, respectively. The activation volume measurements were conducted at similar values of $\dot{\varepsilon}/D_l$, where $\dot{\varepsilon}$ is the

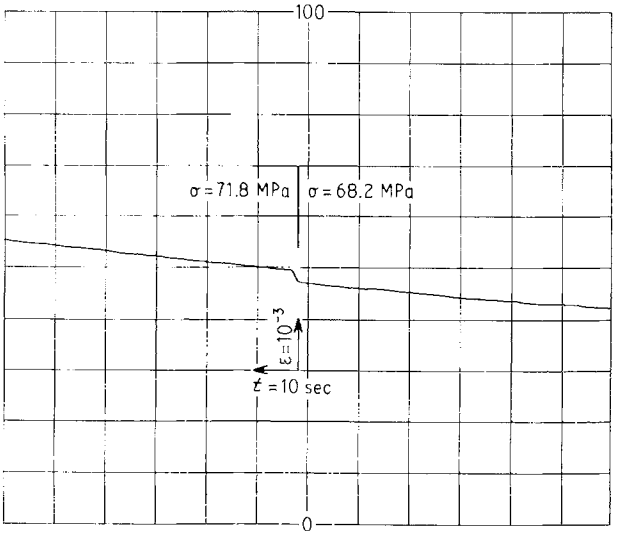


*Figure 1* Chart recording for Cu–30% Zn tested at 673 K showing the effect of a stress increase from 68.2 to 71.8 MPa. $d$ = 120 μm.

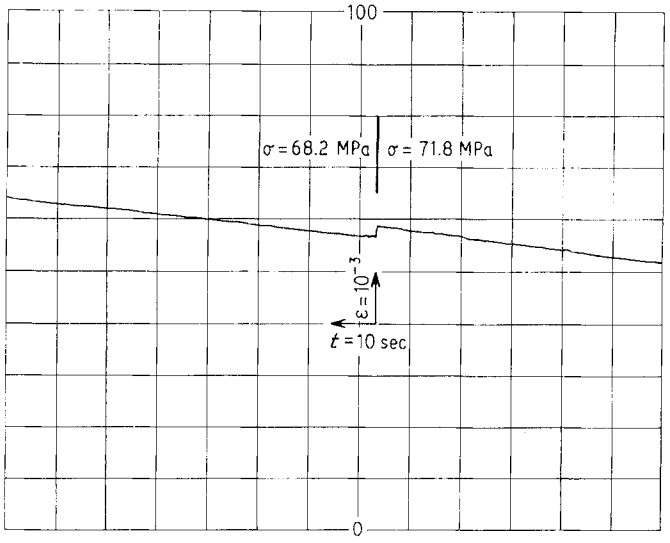


*Figure 2* Chart recording for Cu–30% Zn tested at 673 K showing the effect of a stress decrease from 71.8 to 68.2 MPa. $d = 120\,\mu m$.

creep rate and $D_l$ is the lattice self-diffusion coefficient, for the three materials so as to enable an effective comparison to be made between them. The magnitude of $D_l$ for copper and alpha brass were estimated from a compilation of diffusion data as shown in the Appendix. The stress changes were conducted in both the primary and the secondary creep stages, and $V^*$ was calculated from Equation 4 assuming $\sigma = 2\tau$. The error in the measurement of $V^*$ was estimated to be about 10 to 20%.

## 3. Results

### 3.1. Stress exponents and activation energies for creep

The creep properties of copper and alpha brass are reported elsewhere [10, 11] and only a brief description of these results is given here. The creep data for aluminium also have been reported elsewhere [12]. At temperatures above 573, 723 and 673 K for Al, Cu and Cu–30% Zn, respectively, corresponding to $0.55\,T_m$, the stress exponents were similar and varied between 4.1 and 4.5. Below these temperatures, the stress exponents increased with decreasing temperature reaching about 6.6 at 623 K for copper and 5.4 at 573 K for alpha brass. A value of $n \approx 4.5$ was reported for aluminium in an earlier investigation [12].

Despite the similarities in the magnitudes of the creep stress exponent for copper and alpha brass when $T > 0.55\,T_m$, two major differences were observed in the magnitudes and stress dependence of the true activation energy for creep of these materials determined by plotting the temperature-compensated creep rate against the inverse of the absolute temperature for different values of the normalized stress, $\sigma/G$, where $G$ is the shear modulus (Figs 3 and 4). First, the values of $Q_c$, which varied between 135 and 180 kJ mol$^{-1}$, were always less than the activation energy for lattice diffusion, $Q_l$, for copper, where the average value of $Q_l \approx 210$ kJ mol$^{-1}$ (i.e. $\Delta H_{SD}$) was estimated by compiling diffusion data obtained from several sources [13–17] as shown in the Appendix. In contrast, the magnitudes of $Q_c$ for Cu–30% Zn, which varied between 170 and 180 kJ mol$^{-1}$, were comparable to the activation energies for intrinsic diffusion of copper and zinc in the alloy, as well as with those estimated from Arrhenius-type equations for complex diffusion coefficients, given in the Appendix. Second, the activation energies for copper were linearly dependent on the normalized stress as shown in Fig. 5a, where the horizontal broken line indicates the activation energy for lattice diffusion with $Q_l \approx 210$ kJ mol$^{-1}$. In contrast, the activation energies for the alloy are only weakly dependent on stress as shown in Fig. 5b, where the horizontal broken lines represent the values for intrinsic diffusion of copper and zinc in the alloy.

### 3.2. Variation of the apparent activation volume for creep with strain

Fig. 6 shows the variation of $V^*$ with creep strain for copper. (In this investigation, a value of $b = 2.56 \times$

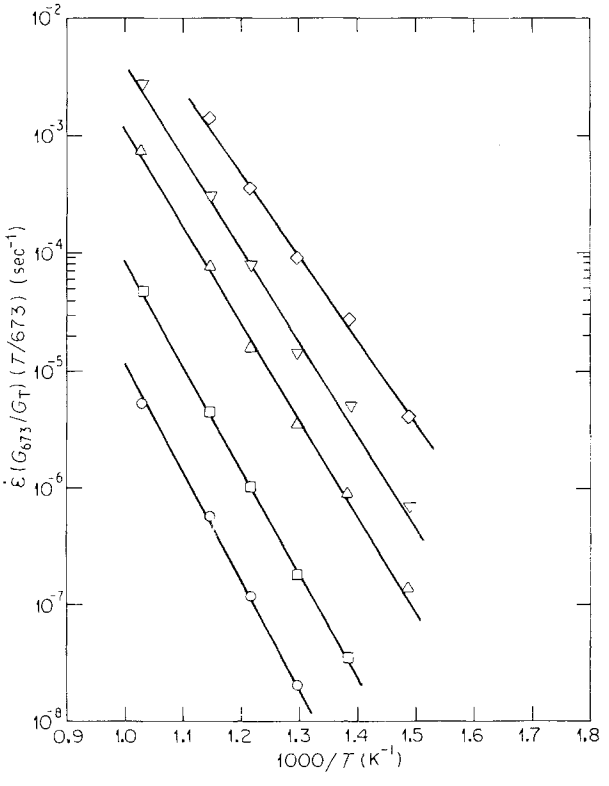


*Figure 3* Temperature compensated steady-state creep rate plotted against the inverse of the absolute temperature for copper. $\sigma/G$ and $Q_c$ (kJ mol$^{-1}$), respectively: (○) $3.0 \times 10^{-4}$, 180 ± 10; (□) $5.0 \times 10^{-4}$, 170 ± 10; (△) $1.0 \times 10^{-3}$, 155 ± 5; (▽) $1.4 \times 10^{-3}$, 150 ± 10; (◇) $2.0 \times 10^{-3}$, 135 ± 10.

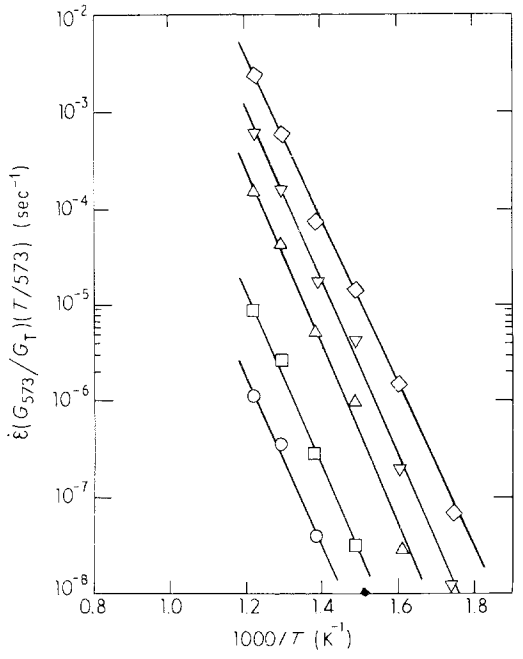


*Figure 4* Temperature compensated steady-state creep rate plotted against the inverse of the absolute temperature for alpha brass. $\sigma/G$ and $Q_c$ (kJ mol$^{-1}$), respectively: (○) $3.0 \times 10^{-4}$, $180 \pm 15$; (□) $5.0 \times 10^{-4}$, $170 \pm 10$; (△) $1.0 \times 10^{-3}$, $155 \pm 5$; (▽) $1.4 \times 10^{-3}$, $1.4 \times 10^{-3}$, $170 \pm 20$; (◇) $2.0 \times 10^{-3}$, $170 \pm 20$.

$10^{-10}$ m was assumed for copper and alpha brass, while $b = 2.86 \times 10^{-10}$ m for aluminium [18].) In general, two modes of behaviour can be noted. First, the apparent activation volume decreases markedly with strain at the lower temperatures and higher stresses with $V^* > 2000\,\boldsymbol{b}^3$ for low strains at 923 K to $V^* \approx 100\,\boldsymbol{b}^3$ when $\varepsilon \approx 4\%$ at 673 K. (The terms "low" and "high" used in this paper refer qualitatively to the lower and higher ranges of stress or temperature, respectively, in which the data were obtained. Thus, "low" and "high" temperatures, which still pertain to the intermediate temperature regime, are used in a relative sense so as to aid in the description of the experimental results.) Second, $V^*$ is essentially independent of strain at the higher temperatures (e.g. 973 K) and at the lower stresses (e.g. 8.92 MPa at 973 K). For the latter conditions, the values of $V^*$ are of the order of 1600 to $1700\,\boldsymbol{b}^3$.

A similar trend is observed in the strain dependence of $V^*$ for Cu–30% Zn (Fig. 7). The two modes of behaviour observed in copper are also seen in this alloy. Once again, a significant decrease in the magnitude of $V^*$ occurs with strain at the lower temperatures and higher stresses with $V^* \approx 1700\,\boldsymbol{b}^3$ for $\varepsilon < 1\%$ at 708 K to $V^* \approx 100\,\boldsymbol{b}^3$ at $\varepsilon > 3\%$ below 708 K. However, the magnitude of $V^*$ attains an approximately constant value of about $400\,\boldsymbol{b}^3$ which is essentially independent of strain for $T \geqslant 773$ K and $\sigma \leqslant 24.6$ MPa.

It appears that the variation of $V^*$ with strain is influenced by the ease of formation of the steady-state substructure because steady-state behaviour was relatively better defined at the higher temperatures and lower stresses for both materials [10, 11].

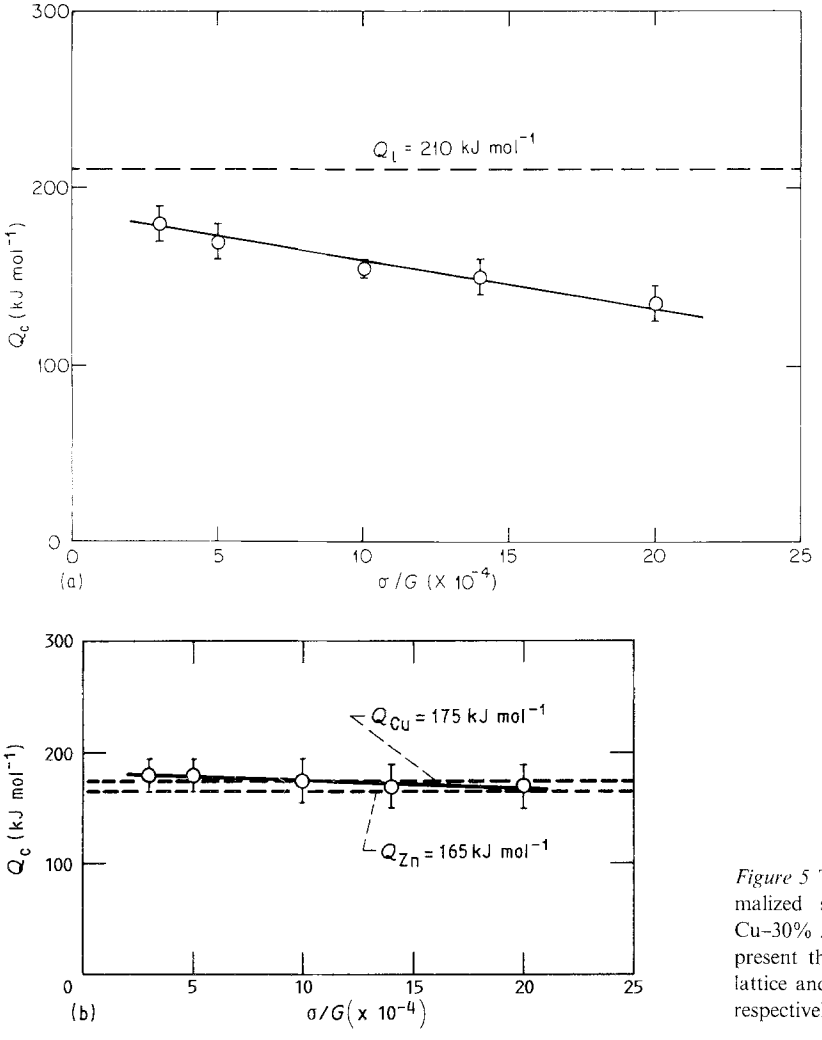


*Figure 5* True activation energy plotted against the normalized stress for (a) copper, $d = 250\,\mu$m, and (b) Cu–30% Zn, $d = 120\,\mu$m. The horizontal broken lines represent the average values of the activation energies for lattice and intrinsic diffusion in the pure metal and alloy, respectively.

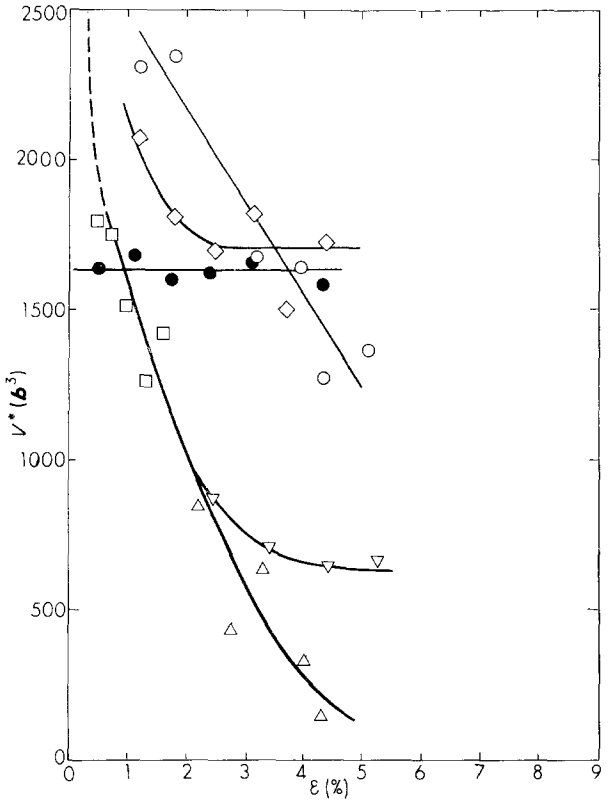


*Figure 6* Apparent activation volume as a function of strain for copper. $d = 250\,\mu m$. $T$ (K) and $\sigma$ (MPa), respectively: (△) 673, 61.0; (▽) 723, 47.3; (□) 773, 24.3; (○) 923, 15.3; (◇) 923, 12.1; (●) 973, 8.92.

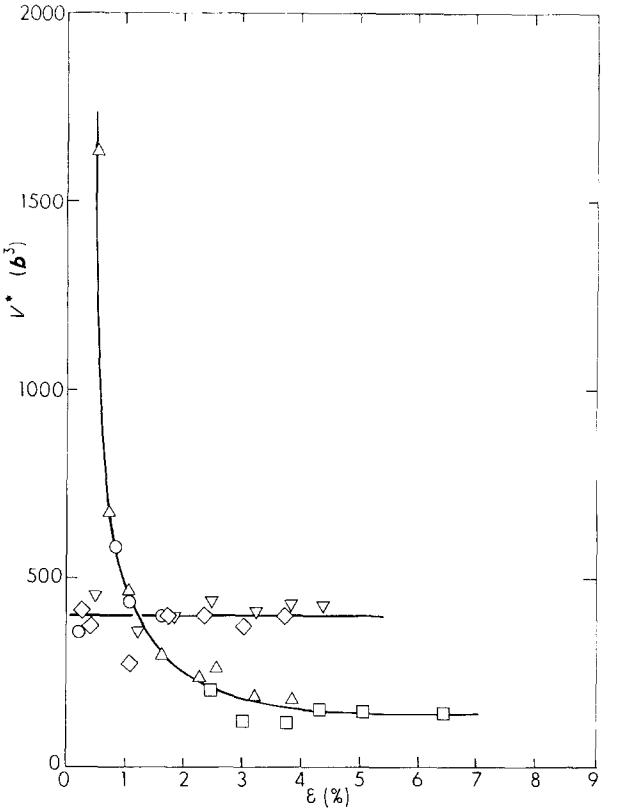


*Figure 7* Apparent activation volume as a function of strain for alpha brass. $d = 120\,\mu m$. $T$ (K) and $\sigma$ (MPa), respectively: (□) 623, 61.5; (△) 708, 37.8; (▽) 773, 24.6; (◇) 773, 23.5; (○) 823, 15.6.

Further support for this viewpoint was obtained from experiments conducted on aluminium under conditions where subgrains develop during creep [12]. For the latter conditions, the magnitude of $V^*$ does not vary significantly with strain once the steady-state substructure has formed; however, it increases markedly with temperature and decreasing stress (Fig. 8).

### 3.3. Variation of the apparent activation volume with stress

In the steady-state region, the apparent activation volume decreases with increasing stress for copper but it appears to be essentially independent of temperature as shown in Fig. 9. Although Li and co-workers [1, 2] suggested that

$$V^* = (2nkT/\sigma) \qquad (5)$$

is applicable in the power-law creep region, estimates of $V^*$ from Equation 5 do not agree with the experimental results reported in the present investigation. For example, the magnitude of $V^*$ calculated from Equation 5 is about $670\,\boldsymbol{b}^3$ at 973 K for $\sigma = 10$ MPa and $n = 4.2$, and this is less than half the experimental values. It appears unlikely that this discrepancy can be attributed entirely to variations in the microstructure following a stress change because the data reported in this paper fall within a relatively narrow scatter band (Figs 6 and 9) irrespective of whether $V^*$ was determined after a stress increase (Fig. 1) or a stress decrease (Fig. 2). However, it is more likely that this discrepancy is related to the higher values of $n$ generally obtained from "constant structure" experiments in comparison to those determined from multiple specimen creep tests [19]. This is evident through a

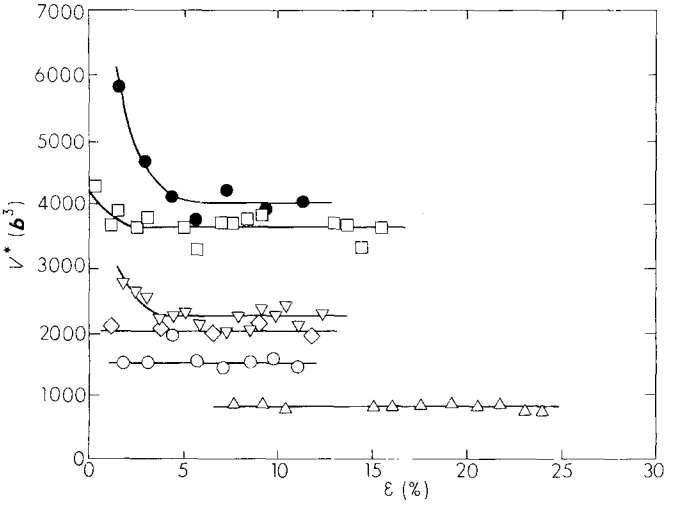


*Figure 8* Apparent activation volume for aluminium plotted against strain. $d = 230\,\mu m$. $T$ (K) and $\sigma$ (MPa), respectively: (△) 510, 22.70; (○) 573, 8.63; (◇) 673, 4.76; (▽) 673, 3.58; (□) 673, 2.70; (●) 673, 2.04.

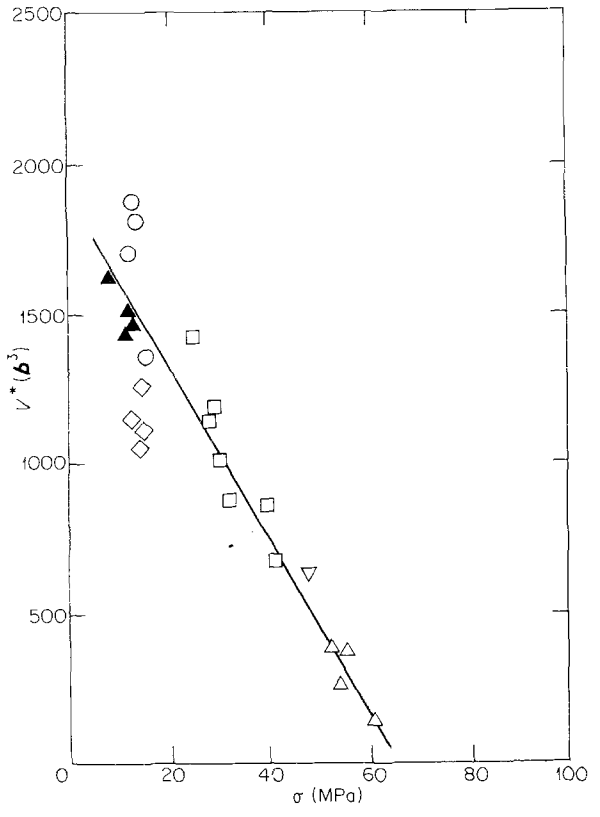


*Figure 9* Apparent activation volume plotted against stress for copper in the steady-state creep regime. $d = 250\,\mu m$. $T$ (K): (△) 673, (▽) 723; (□) 773; (◇) 873; (○) 923; (▲) 973.

comparison of the magnitudes of the stress exponents, where the value of $n \approx 10$ calculated from Equation 5 for $V^* \approx 1600\,\boldsymbol{b}^3$ at 973 K and 10.0 MPa (Fig. 9) is larger than the value of $n \approx 4.2$ determined from multiple specimen creep tests.

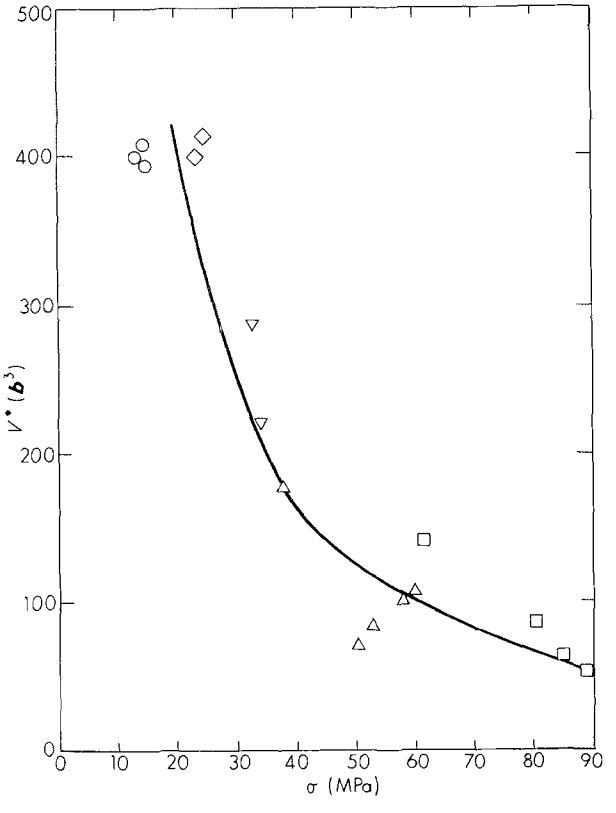


*Figure 10* Apparent activation volume plotted against stress for alpha brass in the steady-state creep regime. $d = 120\,\mu m$. $T$ (K): (□) 626; (△) 707; (▽) 748; (◇) 773; (○) 823.

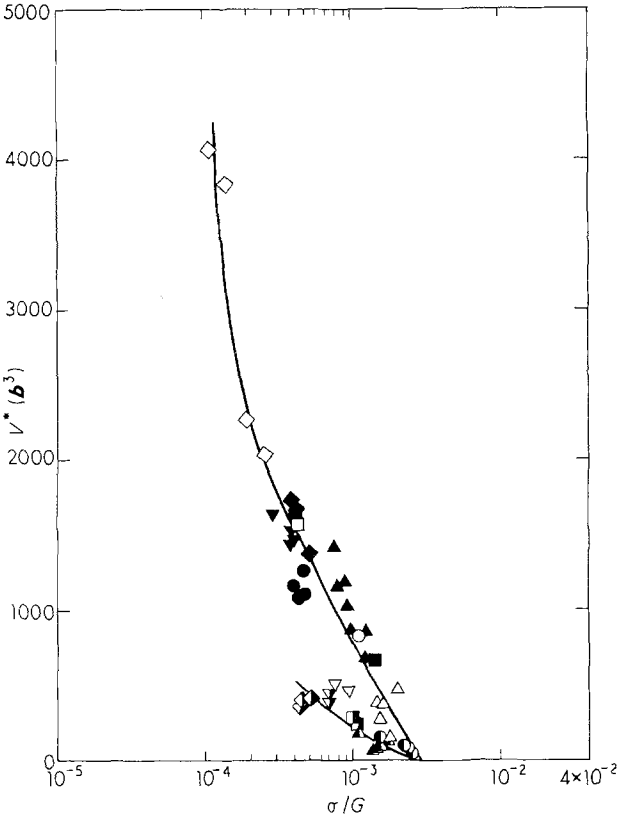


*Figure 11* Variation of the apparent activation volume with normalized stress for aluminium, copper and alpha brass in the steady-state creep region. The data reported by König and Blum [20] for aluminium (▽) were obtained from stress relaxation experiments. $T$(K): Al, (○) 509, (□) 572, (◇) 673, (▽) 523; Cu, (△) 673, (■) 723, (▲) 773, (●) 873, (◆) 923, (▼) 973; Cu–30% Zn, (◐) 626, (◭) 707, (◨) 748, (◬) 773, (◈) 823.

The apparent activation volume also decreases with increasing stress for alpha brass in the steady-state region (Fig. 10), and once again, no significant temperature dependence is observed. In comparison to the results on copper, the magnitudes of $V^*$ estimated from Equation 5 were found to be in reasonable agreement with the experimental values. For instance, Equation 5 gives a value of $V^* \approx 370\,\boldsymbol{b}^3$ at 823 K for $\sigma = 15$ MPa and $n = 4.1$ and this is in excellent agreement with the experimental value of $V^* \approx 400\,\boldsymbol{b}^3$.

Noting that $\Delta G_c = Q_c - T\Delta S_c$, where $\Delta S_c$ is the activation entropy for creep, Equation 4 can be expressed in the form

$$-(\partial Q_c/\partial\sigma)_{P,T} + T(\partial\Delta S_c/\partial\sigma)_{P,T} = V^*/2 \quad (6)$$

assuming $\sigma = 2\tau$. The first term in Equation 6 represents the slope of a plot of $Q_c$ against $\sigma$ such as that shown in Fig. 5. For copper, it follows from Fig. 5a that this term is a constant equal to about $75\,\boldsymbol{b}^3$ at 775 K, so that the stress dependence of $V^*$ shown in Fig. 9 can be attributed entirely to the stress dependence of the second term. This conclusion is equally valid for alpha brass because $Q_c$ is only slightly dependent on stress with $(\partial Q_c/\partial\sigma)_{P,T} \approx 20\,\boldsymbol{b}^3$ (Fig. 5b). In addition, it follows from Equation 6 that the second term is also inversely dependent on temperature because $Q_c$ and $V^*$ are not strongly temperature dependent.

In Fig. 11, the apparent activation volume is plotted against the normalized stress semi-logarithmically for the three materials studied in this investigation. The experimental data lie on a single curve for the pure metals and the magnitude of $V^*$ is significantly higher than those for the alloy for $\sigma/G \leqslant 10^{-3}$. The data obtained by König and Blum [20] on aluminium are also shown for comparison. The latter results were determined by the stress relaxation technique, and the values are lower than those obtained in the present investigation by about 50%. This difference between the two experimental results can be attributed partly to error in measurement, which is estimated to be about 10 to 20% in the present investigation, and partly to the greater influence of recovery during stress relaxation as compared to the stress change technique employed in the present investigation [20, 21]. The latter argument is substantiated by a previous investigation by Hausselt [21] who showed that the values of $V^*$ determined by the stress relaxation technique are about 10 to 20% lower than those obtained from stress change experiments owing to a greater degree of recovery associated with the former method.

## 4. Discussion

### 4.1. Low-temperature behaviour

The variation of $V^*$ with strain at the lower temperatures and higher stresses (Figs 4 and 5) is significant because it suggests a corresponding change in the obstacle spacing, $l^*$, or the obstacle width, $d^*$, through the relation $V^* = bl^*d^*$.The obstacle width is expected to be only slightly dependent on stress [20] so that it may be assumed to be approximately constant. For these conditions, the stress and strain dependence of $V^*$ can be attributed entirely to their effect on the obstacle spacing.

The decrease in $V^*$ with increasing strain (Figs 6 and 7) suggests an increase in the obstacle density, $\varrho$, where the nature of the obstacle may be immobile dislocations or dislocation dipoles [5]. Noting that $l^* \approx \varrho^{-1/2} \propto (G/\sigma)$, it is expected that $V^* \propto (G/\sigma)$. A power-law regression fit to the data shown in Fig. 7 for copper suggested that

$$V^* = 5\boldsymbol{b}^3 (G/\sigma)^{0.7} \quad (8)$$

The conclusion drawn here, that the creep mechanism dominant at the lower temperatures and higher stresses is determined by the rate of intersection of obstacles, finds further support from the expected magnitudes of $V^*$ which should range between $10^2$ and $10^4\,\boldsymbol{b}^3$ [5, 22]. A detailed observation of slip-line morphology at the surface of pre-polished specimens, and an analysis of the creep data were also found to be consistent with this conclusion [11]. Although the present discussion has been limited to the $V^*$ data obtained on copper, a similar conclusion appears to be valid for alpha brass for which the magnitudes of $V^*$ and its decrease with increasing strain (Fig. 7) are suggestive of the dominance of an obstacle glide-controlled process. This suggestion is consistent with the fact that the creep data at the lower temperatures and higher stresses could also be represented by an exponential relation in addition to the power-law creep equation [11].

### 4.2. High-temperature behaviour

An analysis of the creep data showed that the contributions from dislocation climb was quite significant at the higher temperatures and lower stresses for copper and alpha brass [11]. An additional contribution resulting from the presence of solutes around dislocations also appears to play an important role in governing the creep behaviour of the alloy for certain conditions. This latter point is addressed later on, and for the present, only the nature of the rate-controlling mechanism operating in the pure metal is considered.

The increasing importance of dislocation climb at the higher temperatures and lower stresses is reflected in the relative independence of $V^*$ on strain (Figs 6 and 8). Similar observations have also been reported for alpha iron [23] and magnesium [24]. As reported in Section 3.2, the magnitude of $V^*$ measured for copper at the higher temperatures and lower stresses was about 1600 to $1700\,\boldsymbol{b}^3$, and this is much larger than the expected value of about $1\,\boldsymbol{b}^3$ associated with the climb of a single-edge dislocation [5, 22]. Instead, the climb process appears to involve the nonconservative motion of jogs on screw dislocations for which the expected values of $V^*$ are between $10^2$ and $10^4\,\boldsymbol{b}^3$ [5, 22].

For alpha brass, $V^*$ is also essentially independent of strain at the higher temperatures and lower stresses (Fig. 7). Similar observations have also been reported for other alloys: Al–9.5 at % Zn [25], Al–11% Zn [20], Mg–0.8% Al [26], and AlCuNiCo [27]. It is interesting to note that the value of $V^* \approx 400\,\boldsymbol{b}^3$ observed under these conditions for Cu–30% Zn is similar to those reported for Al–Mg [2] and Al–Zn [21, 25] despite the fact that the latter two alloys exhibit class A and class M behaviour, respectively. The magnitude of $V^*$ for alpha brass is in agreement with the expected values of 1 to $10^3\,\boldsymbol{b}^3$ for a solute drag-controlled mechanism [5] as well as with those associated with the nonconservative motion of jogs on screw dislocations.

Although the apparent activation volume data, taken together with values of $n \approx 4.2$ and $Q_c \approx 170 - 180\,\mathrm{kJ\,mol^{-1}}$, suggest that dislocation climb is the rate-controlling mechanism in alpha brass at these temperatures and stresses, the role of solute drag-controlled dislocation glide cannot be entirely ruled out for several reasons. First, the observed magnitudes of $Q_c$ are also in reasonable agreement with those estimated from complex diffusion equations for a solute drag-limited glide process in Cu–30% Zn [11]. Second, sigmoidal and inverse transients have been observed in this material during primary creep [11, 28, 29]. Third, the characteristics of the strain transients after stress changes suggest the importance of solute drag on dislocation motion [30]. Fourth, the magnitudes of the instantaneous strain observed in stress increase and stress decrease type experiments were found to be about the same [11], similar to the observations reported on Al–Mg alloys [31–33] which are known to exhibit class A behaviour. Therefore, it appears that both dislocation climb and viscous glide govern the creep properties of this alloy. Further support for these conclusions were obtained through an analysis of the creep data on Cu–30% Zn and these are reported elsewhere [11].

## 5. Conclusions

1. At the lower temperatures and higher stresses, $V^*$ decreases markedly with increasing strain for copper and alpha brass, but it is essentially independent of strain at the higher temperatures and lower stresses.

2. The magnitude of $V^*$ decreases with increasing stress for copper and alpha brass in the region of steady-state creep but it is independent of temperature for both materials. These results are attributed to the stress and temperature dependence of the activation entropy for creep.

3. The observations at the lower temperatures and higher stresses are consistent with the characteristics of obstacle-controlled dislocation glide. At higher temperatures and lower stresses, the magnitude of $V^*$ suggests that dislocation climb, involving the non-conservative motion of jogs on screw dislocations, becomes important. An additional contribution from solute drag mechanisms also appears to be important in alpha brass.


## Acknowledgements

The author thanks Professor T. G. Langdon of the University of Southern California for the use of his research facilities and for providing the materials used in this investigation. Financial support for this study was provided in part by the United States Department of Energy and in part by the NASA Lewis Research Center.


## Appendix

The activation energy for lattice self-diffusion in copper was estimated by re-plotting the diffusion data obtained from several sources [13–17] (Fig. A1). A linear regression fit suggested that the data are well represented by

$$D_l = 6.1 \times 10^{-5} \exp(-210/RT)\ \mathrm{m^2\,sec^{-1}} \quad \text{(A1)}$$

where $R$ is the universal gas constant equal to $0.0083\ \mathrm{kJ\,mol^{-1}}$.

The intrinsic diffusion coefficients for copper and zinc in Cu–30% Zn were estimated by re-plotting diffusion data obtained from several sources [13, 34, 35] (Fig. A2). The experimental data are in good agreement with the expressions

$$D_{Cu} = 8.4 \times 10^{-5} \exp(-175/RT)\ \mathrm{m^2\,sec^{-1}} \quad \text{(A2)}$$

$$D_{Zn} = 1.0 \times 10^{-4} \exp(-165/RT)\ \mathrm{m^2\,sec^{-1}} \quad \text{(A3)}$$

The tracer diffusion data were converted to intrinsic diffusion coefficients through the relation

$$D_i = D_i^* [1 + \mathrm{d}(\ln \gamma_i)/\mathrm{d}(\ln N_i)] \quad \text{(A4)}$$

where $D_i$ and $D_i^*$ are the intrinsic and tracer diffusion coefficients of the $i$th species, respectively, $\gamma_i$ its activity coefficient in the alloy, and $N_i$ is the atom fraction of the $i$th component. The value of $\mathrm{d}(\ln \gamma_i)/\mathrm{d}(\ln N_i)$ was obtained from a plot of experimental values of $\gamma_{Zn}$ against $N_{Zn}$ based on the data reported by Fisher *et al.* [36].

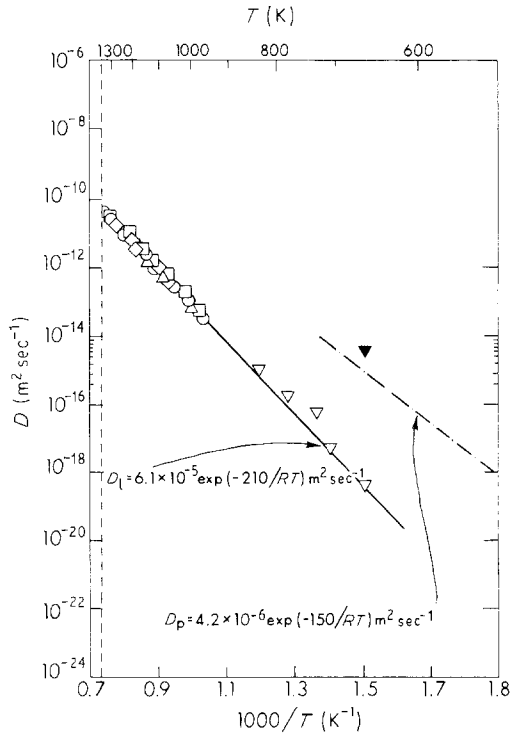


*Figure A1* Plot of the lattice diffusion coefficient against the inverse of the absolute temperature for copper. The diffusion data were obtained from several sources [13–17]. The expected trend for the temperature dependence of the dislocation pipe diffusion coefficient, $D_p$, is also shown for comparison, and this equation and the single datum point are based on the investigation by Bowden and Balluffi [15]. Method: (◇) tracer [13], (□) tracer [14], (▼, ▽) void shrink [15], (○) tracer [16], (△) tracer [17]. Open symbols, $D_l$; solid symbols, $D_p$.

Although the expressions for intrinsic diffusion coefficient given by Equations A2 and A3 are simple to use, they are not always suitable for analysing creep data of binary solid solution alloys because both diffusing species can contribute to the dominant creep

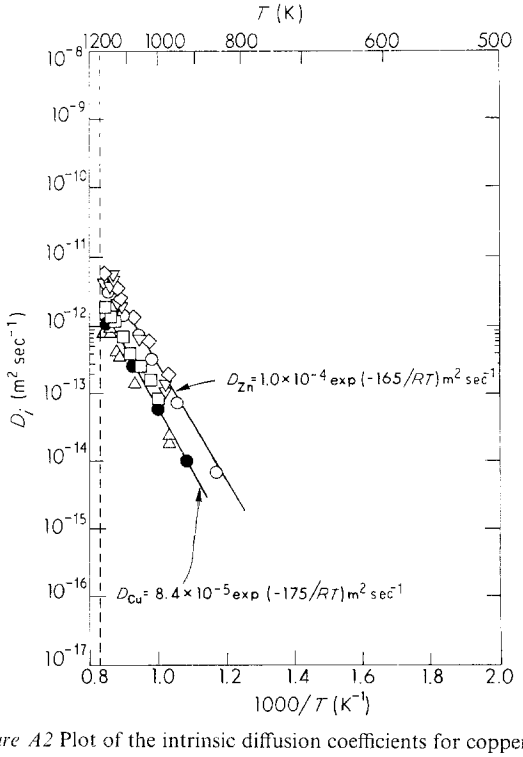


*Figure A2* Plot of the intrinsic diffusion coefficients for copper and zinc in Cu–30% Zn against the inverse of the absolute temperature. (△, ○, □) $D_{Cu}$, (▽, ○, ◇) $D_{Zn}$. Method: (□, ◇) tracer [13]; (△, ▽) diffusion couple [34]; (●, ○) tracer [35].

mechanism. For these conditions, Fuentes-Samaniego *et al.* [37–39] have proposed

$$\tilde{D}_c = (N_{Cu} D^*_{Cu} + N_{Zn} D^*_{Zn})/f_0 \quad \text{(A5)}$$

where $\tilde{D}_c$ is the complex diffusion coefficient when dislocation climb is dominant and $f_0$ is a correlation factor equal to 0.78 for fcc alloys, and

$$\tilde{D}_g = [D^*_{Cu} D^*_{Zn}/(N_{Cu} D^*_{Cu} + N_{Zn} D^*_{Zn})] \times [1 + \mathrm{d}(\ln \gamma_{Zn})/\mathrm{d}(\ln N_{Zn})] \quad \text{(A6)}$$

where $\tilde{D}_g$ is the complex diffusion coefficient when viscous glide is the rate-controlling process. Using Equations A5 and A6, plots of $\tilde{D}_c$ and $\tilde{D}_g$ against the inverse of the absolute temperature, and tracer diffusion data reported by Anusavice and co-workers [13, 40] and Hino *et al.* [35], the complex diffusion coefficients for climb and viscous glide-controlled processes are given by

$$\tilde{D}_c = 1.5 \times 10^{-4} \exp(-180/RT)\ \mathrm{m^2\ sec^{-1}} \quad \text{(A7)}$$

$$\tilde{D}_g = 1.5 \times 10^{-4} \exp(-180/RT)\ \mathrm{m^2\ sec^{-1}} \quad \text{(A8)}$$

## References


1. J. C. M. LI, in "Dislocation Dynamics", edited by A. R. Rosenfield, G. T. Hahn, A. L. Bement, Jr and R. L. Jaffee (McGraw-Hill, New York, 1968) p. 87.
2. N. BALASUBRAMANIAN and J. C. M. LI, *J. Mater Sci.* **5** (1970) 434.
3. *Idem, ibid.* **5** (1970) 839.
4. J. C. M. LI, *Canad. J. Phys.* **45** (1967) 493.
5. A. G. EVANS and R. D. RAWLINGS, *Phys. Status Solidi* **34** (1969) 9.
6. O. D. SHERBY and P. M. BURKE, *Prog. Mater. Sci.* **13** (1967) 325.
7. O. D. SHERBY, J. L. ROBBINS and A. GOLDBERG, *J. Appl. Phys.* **41** (1970) 3961.
8. O. D. SHERBY and J. WEERTMAN, *Acta Metall.* **27** (1979) 387.
9. S. V. RAJ, *Scripta Metall.* **20** (1986) 1333.
10. S. V. RAJ and T. G. LANGDON, *Acta Metall.* **37** (1989) 843.
11. S. V. RAJ, PhD thesis, University of Southern California, Los Angeles (1984).
12. R. B. VASTAVA and T. G. LANGDON, in "Advances in Materials Technology in the Americas— 1980", Vol. 2, edited by I. Le May (American Society of Mechanical Engineers, New York, 1980) p. 61.
13. K. J. ANUSAVICE and R. T. DeHOFF, *Metall. Trans.* **30** (1972) 1279.
14. M. BEYELER and Y. ADDA, *J. Physique* **29** (1968) 345.
15. H. G. BOWDEN and R. W. BALLUFFI, *Phil. Mag.* **13** (1969) 1001.
16. S. J. ROTHMAN and N. L. PETERSON, *Phys. Status Solidi* **35** (1972) 305.
17. K. HOSHINO, Y. IIJIMA and K. I. HIRANO, *Acta. Metall.* **30** (1982) 265.
18. H. J. FROST and M. F. ASHBY, in "Deformation-Mechanism Maps: The Plasticity and Creep of Metals and Ceramics" (Pergamon, Oxford, 1982).
19. J. D. PARKER and B. WILSHIRE, *Phil. Mag.* **34** (1976) 485.
20. G. KÖNIG and W. BLUM, *Acta Metall.* **25** (1977) 1531.
21. J. HAUSSELT, *Scripta Metall.* **10** (1976) 565.
22. H. CONRAD, *J. Metals* **16** (1964) 582.
23. M. PAHUTOVÁ, J. ČADEK and P. RYŠ, *Scripta Metall.* **5** (1971) 137.
24. S. VAGARALI and T. G. LANGDON, *Acta Metall.* **29** (1981) 1969.
25. K. KUCHAŘOVÁ and J. ČADEK, *Phys. Status Solidi* **6** (1971) 33.
26. S. S. VAGARALI and T. G. LANGDON, *Acta Metall.* **30** (1982) 1157.
27. W. BLUM and R. SINGER, *Z. Metallkde* **71** (1980) 312.
28. W. J. EVANS and B. WILSHIRE, *Metall. Trans.* **1** (1970) 2133.
29. *Idem, Scripta Metall.* **8** (1974) 497.
30. S. V. RAJ, *ibid.* **20** (1986) 1751.
31. H. OIKAWA and K. SUGAWARA, *ibid.* **12** (1978) 85.
32. H. OIKAWA, *Phil. Mag.* **37** (1978) 707.
33. T. G. LANGDON and P. YAVARI, in "Creep and Fracture of Engineering Materials and Structures", edited by B. Wilshire and D. R. Owen (Pineridge Press, Swansea, 1981) p. 71.
34. R. RESNICK and R. W. BALLUFFI, *Trans. AIME* **203** (1955) 1004.
35. J. HINO, C. TOMIZUKA and C. WERT, *Acta Metall.* **5** (1957) 41.
36. J. C. FISHER, J. H. HOLLOMON and D. TURNBULL, *Trans. AIME* **175** (1948) 202.
37. R. FUENTES-SAMANIEGO, W. D. NIX and G. M. POUND, *Phil. Mag.* **42A** (1980) 591.
38. R. FUENTES-SAMANIEGO and W. D. NIX, *Scripta Metall.* **15** (1981) 15.
39. R. FUENTES-SAMANIEGO, W. D. NIX and G. M. POUND, *Acta Metall.* **29** (1987) 487.
40. R. T. DeHOFF, A. G. GUY, K. J. ANUSAVICE and T. B. LINDEMER, *Trans. AIME* **236** (1966) 881.



*Received 20 June*
*and accepted 7 December 1988*